Immunodetection of Urinary C-terminal Telopeptide Fragment of Type II Collagen: An Osteoarthritis Biomarker Analysis

Shuwei Wang[1], Shanlin Su[1], Chunyun Yu[1], Subash C.B. Gopinath[2,3], Zhiquan Yang[1*]

[1]Department of Orthopedics, Shouguang Hospital of TCM, No.3353, Holy City Street, Weifang, Shandong Province, 262700, China
[2]School of Bioprocess Engineering, 02600 Arau, [3]Institute of Nano Electronic Engineering, 01000 Kangar, Universiti Malaysia Perlis, Perlis, Malaysia.

Highlights

This study reports a sensing strategy with antibody conjugated gold nanoparticle on Interdigitated electrode to determine Urinary C-terminal telopeptide fragment of type II collagen-II. This strategy was improved the detection by attracting higher uCTX-II molecules and the detection limit falls in the range of 10 to 100 pM with the sensitivity at 10 pM.

Shuwei Wang: doctorwsw@sina.com
Shanlin Su: sushanlin1@sina.com
Chunyun Yu: yuchunyun90@sina.com
Subash C.B. Gopinath: subash@unimap.edu.my
Zhiquan Yang: yangzhiquan75@sina.com

***Correspondence to:** yangzhiquan75@sina.com

This article has been accepted for publication and undergone full peer review but has not been through the copyediting, typesetting, pagination and proofreading process, which may lead to differences between this version and the Version of Record. Please cite this article as doi: 10.1002/bab.1981.

Abstract

Urinary C-terminal telopeptide fragment of type II collagen (uCTX-II) has been reported as the efficient blood-based biomarker for osteoarthritis, affects knees, hands, spine and hips. This study reports a sensing strategy with antibody conjugated gold nanoparticle (GNP) on Interdigitated electrode (IDE) to determine uCTX-II. GNP-antibody complex was chemically immobilized on IDE surface through the amine linker. uCTX-II was determined by monitoring the alteration in current upon interacting GNP complexed antibody. This strategy was improved the detection by attracting higher uCTX-II molecules and the detection limit falls in the range of 10 to 100 pM with an acceptable regression values [y = 0.6254x - 0.4073 R^2 = 0.9787]. The sensitivity of the detection was recognized at 10 pM. Additionally, upon increasing uCTX-II concentration, the current changes were increased in a linear fashion. Control detection with non-immune antibody and control protein do not increase the current level, confirming the specific detection of uCTX-II. This method of detection helps to diagnose osteoarthritis and its follow-up treatment.

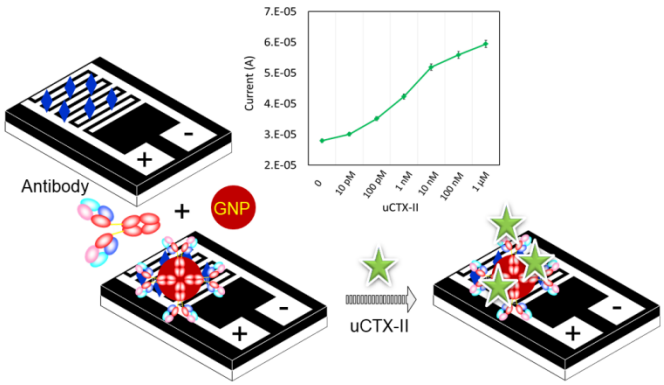

Keywords

Osteoarthritis; Interdigitated electrode; Gold nanoparticle; Biosensor; antibody

1. Introduction

Osteoarthritis is an age-related chronic disorder with the condition of breaking down of the protective tissue cartilage in the bones. It primarily affects the joint bones in hands, knees, hips and spine, cause the stiffness and pains [1]. Osteoarthritis mainly affects the aged people, identifying and treating osteoarthritis is mandatory to give a quality life to the older people [2]. Until now, the methods of radiographic and computer tomography are used to identify the damage in the cartilage and measure

the joint space width [3], however, this method has some limitations to identify. Blood based biomarker helps to detect the changes with Osteoarthritis at its earlier stages with more sensitivity and reliable [4]. Urinary C-terminal telopeptide fragment of type II collagen (uCTX-II) has been found as one of the potential biomarkers for osteoarthritis [5,6]. The level of uCTX-II was found to enhance with disease condition, in which there is elevated cartilage turnovers, such as rheumatoid arthritis and osteoarthritis [7,8]. This research was focused to determine and quantify the level of uCTX-II by conducting immunoassay with the specific antibody for uCTX-II on Interdigitated electrode (IDE) biosensor.

IDE sensors have been widely recognized as the potential system, applied in the medical diagnosis. IDE uses di- or tri-electrodes with the properly aligned gap and finger regions to be parallel or concentric. Under bare condition (no surface modification), it shows a minimum electric flow on dielectrode system. When the surface chemical or biological modifications occur, there will be obvious changes in the flow of current to be measured as the biosensor. Biosensor is the process of identifying the targets through the process of interacting biomolecules into a readable signal for diagnosing various kinds of diseases [9–12]. Different sensors, targets and probes have been utilized to detect the small molecule to the intact bacteria or virus [13–15]. Electrochemical sensor is one of the well-established biosensors in this flow, having the higher sensitivity of identifying biomolecules by measuring the biological interactions and converts them into the electrical signal. For a high sensitive detection, optimization of electric coupling between IDE fingers and gaps are mandatory [16,17]. This work was used IDE to reach the maximum

interaction of antibody and uCTX-II. Further, for obtaining the enhanced uCTX-II detection, antibody was conjugated with GNP and immobilized on IDE sensor.

The extensive application of metallic nanoparticle in biosensing purposes has been fortified by their low ratio of size to volume and the exceptional stability at extreme temperatures [18–20]. In particular, GNPs have a high amenability in terms of synthesis and efficiency, minimized cytotoxicity and easy detection [21,22]. Among other metallic nanoparticles, gold nanoparticle is one of the most acceptable due to their unique physical and chemical features. Additionally, GNP maintained a good colloidal stability when submitted for re-dispersion and ultracentrifugation processes. Various applications of GNPs involve for the purpose as antitumor, gene-delivery, cancer therapy, drug-delivery, catalytic, antioxidant, antimicrobial agents and enhancing the analytical performances. Other applications of GNP are in biosensor, electronic devices, conducting element, smart-paper and textiles and Surface-enhanced Raman Spectroscopy [23,24]. Considering all these positive features of GNP, antibody was attached on the surface of GNP and utilized for improving the determination of uCTX-II.

2. Materials and methods

2.1. Chemicals and biomolecules

Phosphate Buffer Solution (pH 7.4; PBS), uCTX-II and anti-uCTX-II antibody were from kit bought in Immunodiagnostic Systems Inc. (UK). Gold nanoparticle was received from Nanocs, USA. Ethanolamine was obtained from Fisher Scientific (USA) and N-hydroxysuccinimide (NHS) and N-ethyl-N'-(3-dimethylaminopropyl)carbodiimide hydrochloride (EDC) were purchased from GE

Healthcare (USA). 16-mercaptoundecanoic acid (16-MDA) was from Sigma Aldrich (USA).

2.2. Interdigitated electrode preparation process

Interdigitated electrode (IDE) fabrication was processed by utilizing the traditional wet etching method [25]. The IDE base with silica wafer was cleaned utilizing the solutions of RCA1 and RCA2 to reduce the unnecessary deposit on the wafer surface. Further the wafer was processed at 500 °C (thermal oxidation) for 1 h to oxidize the wafer layer and the silicon dioxide layer was formed. On the oxidized layer aluminium coil was used to deposit using the thermal evaporator. The conventional photolithography method was used to create the electrode pattern on the aluminium substrate. Further, UV light was exposed on the substrate to transfer the IDE pattern onto the photoresist. The unexposed area of IDE was eliminated by dipping the substrate in the photoresist developer and the moisture content was removed by baking the substrate at 110°C (1 min). In the final step, the unexposed layer of aluminium was etched by dipping IDE in etchant solution. The prepared IDE was cleaned with acetone, followed by distilled water and kept in the dry cabinet. The IDE surface profile was monitored under 3D-nanoprofiler for the confirmation.

2.3. Conjugation of antibody and GNP

Anti-uCTX-II was attached on GNP surface through the chemical linker, 16-MDA (5 mM). Before this process, 16-MDA was mixed with GNP for 1 h at RT, and then unattached 16-MDA was removed and discarded by centrifugation. The 16-MDA conjugated GNP was activated and stabilized by EDC and NHS. And then, activated 16-MDA complex was mixed with 400 nM of anti-uCTX-II and kept for 1 h (RT). The excess antibodies were separated

by centrifugation with the speed of 10,000xg (5 min). The excess antibodies with GNP conjugation were cleaned with distilled water in order to separate the bound antibody with GNP and kept at 4°C, then utilized whenever necessary.

2.4. Biofunctionalization on IDE

Antibody-GNP was attached on IDE through amine linker on APTES. The surface of IDE was initially cleaned by 1% KOH for 1 min and then washed with distilled water to clear the excess KOH. And then, 1% APTES was added on KOH treated IDE surface and rest for 2 hr. Then APTES modified surface was washed thrice with diluted ethanol to remove the excess APTES. The antibody-GNP conjugation was placed for 1 h on the APTES modified surface to get the interaction of GNP with APTES. Finally, antibody-GNP sensor was washed with buffer to clear the excess amount of antibody. Thee antibody-GNP prepared surface was utilized to identify and quantify the level of uCTX.

2.5. Detection of uCTX-II on antibody-GNP immobilized IDE

uCTX was detected on antibody-GNP modified IDE surface. Prior to this experiment, the uncovered IDE was covered with 1 M of diluted ethanolamine. After the blocking, 1 μM of uCTX was interacted and the current changes were noted before and after the addition of uCTX. The difference in current was considered as the interaction of antibody with uCTX.

2.6. Detection limit of uCTX-II on antibody-GNP modified IDE

To evaluate the limit of uCTX interaction with its antibody, various concentrations (10 pM to 100 nM) was diluted in PBS buffer and interacted individually on antibody-GNP modified IDE. For each concentration of uCTX, the current changes were

registered before and after interaction. The difference in current changes was plotted in an excel sheet to calculate the sensitivity and the limit of detection.

2.7. Control experiment on antibody-GNP modified IDE surface

Control experiment was conducted on IDE to identify the specific detection of uCTX. Two experiments namely, (i) non-immune antibody instead of anti-uCTX antibody; (ii) control protein (albumin) instead of uCTX, are conducted on IDE surface. The changes in current were registered before and after immobilization of the biomolecules.

3. Results and discussion

Figure 1 indicates the schematic presentation of uCTX detection on antibody-GNP immobilized IDE. The fabricated surface was monitored under 3D-nanoprofiler and confirmed the uniformly fabricated finger and gap regions (Figure 1; inset). Initially, the surface of IDE was converted into amine through APTES chemical linker. Before this process IDE surface was hydroxylated by using 1% KOH. APTES is perfectly adsorbing on -OH terminated sensing substrate, a complete area of coverage can be obtained for AuNPs. Under this process, each Si bond from APTES will be bonded covalently to the oxygen on the SiO_2 to form a tripod fashion with increased amino groups oriented from the surface to be bonded with GNPs [26]. In this work, higher antibody-GNP conjugation was populated on IDE through the APTES linker. On these antibodies modified surfaces, the target of uCTX was added. Depends on the interaction of uCTX with its antibodies, the current flow has been changed. The changes in current flow were recorded to detect and quantify the levels of uCTX.

3.1. Surface functionalization with antibody-GNP on IDE

Surface functionalization of antibody-GNP was performed on IDE through the APTES linker to detect uCTX. The current changes for each immobilization process were recoded to confirm the binding of biomolecules. As shown in figure 2a, bare OH treated IDE displays the current level as 1.6 E-08 A, after adding APTES, the current response was enhanced to 4.31E-07 A. This current change attested the binding of APTES on OH-modified IDE sensor surface. After that, when antibody-GNP conjugation was added, the current was further enhanced to 2.49E-05 A. The difference in current of before and after antibody immobilization was found as 24.5 E-06 A (Figure 2b). This higher difference in current changes was due to the higher number of antibody-GNP immobilizations on APTES modified IDE surface. Further, the excess surface was covered by ethanolamine to be blocker. Only a small current change was registered after adding the ethanolamine due to the occupation of antibody-GNP on IDE surface, indicating only small portion left for ethanolamine coverage.

3.2. Detection of uCTX by GNP-conjugated antibody

uCTX was detected on IDE surface by using the interaction of uCTX and antibody-GNP. Initially, 1 μM of uCTX was placed on ethanolamine blocked surfaces. The current was enhanced from 2.49 E-05 to 6.55 E-05 A (Figure 3a). This current alteration was attested the interaction of uCTX with its antibody. Since higher numbers of antibodies were attached on the surface of the GNP, it provides more opportunities to attract larger numbers of uCTX. This improves the detection strategy for uCTX identification.

3.3. Limit of detection of uCTX by GNP-conjugated antibody

Detection limit for uCTX interaction with its antibody was calculated by titrating different concentrations of uCTX and added individually on antibody-GNP modified surfaces. As indicated in figure 3b, after adding 10 pM of uCTX, the current was enhanced from 2.49 E-05 to 3.01E-05 A. There is not much difference was noted after adding 10 pM of uCTX. Increasing uCTX concentration to 100 pM, current was increased to 3.51E-05 A. Further increment in the concentration of uCTX to 1 nM, 10 nM, and 100 nM, the current levels were gradually increased to 4.24 E-05, 5.19 E-05, and 5.59 E-05 A, respectively (Figure 4a). The differences in current of before and after adding uCTX for 10 pM, 100 pM, 1 nM, 10 nM and 100 nM were calculated as 0.21, 0.71, 1.44, 2.39 and 2.79 E-05 A, respectively. The limit of detection was calculated with the lowest concentration of uCTX on the calibration line versus the background signal (standard deviation of the baseline + 3σ). The sensitivity falls with the apparent difference between lower concentrations. From the linear regression graph, the detection limit of uCTX was measured as in the range of 10 to 100 pM by considering 3σ estimation (*n=3*) (Figure 4b). From the obtained results, the sensitivity was predicted to be 10 pM.

3.4. Selective detection of uCTX on IDE surface

Two different control experiments were conducted namely, (i) with non-immune antibody instead of uCTX antibody and (ii) control protein (albumin) instead of uCTX. As shown in figure 5, control experiments were failed to increase the current changes, while the specific experiment was clearly displayed the changes of current. This result indicates the selective determination of uCTX on antibody-GNP modified IDE sensing surface.

4. Conclusion

Diagnosing osteoarthritis by a suitable biomarker is necessary to yield the proper treatment with the fast recovery. uCTX has been found to be a potential biomarker for osteoarthritis, this research was focused to estimate the level of osteoarthritis severity by using the interdigitated electrode sensor (IDE). Antibody-conjugated gold nanoparticle (GNP) was immobilized on IDE surface to enhance the detection of uCTX. The detection limit of uCTX was found in the range between 10 and 100 pM. Apart from that the current response was gradually enhanced when increase the concentration of uCTX. Control experiments with non-immune antibody and albumin do not show any specific response, indicating the specific detection of uCTX. This antibody-GNP conjugated electrochemical sensor helps to diagnose the osteoarthritis.

Competing interests

The authors declare that they have no competing interests.

Author Contributions

Shuwei Wang: Investigation; Methodology; Conceptualization; Data Curation; Writing—original draft; Writing-Reviewing and Editing.
Shanlin Su: Visualization; Validation; Formal analysis; Writing-Reviewing and Editing.
Chunyun Yu: Data Curation; Visualization; Writing-Reviewing and Editing.
Subash C.B. Gopinath: Data Curation; Writing—original draft; Writing-Reviewing and Editing
Zhiquan Yang: Visualization; Supervision; Data Curation; Funding; Writing-Reviewing and Editing

References

[1] Stolz, M., Gottardi, R., Raiteri, R., Miot, S., et al., 2009. Early detection of aging cartilage and osteoarthritis in mice and patient samples using atomic force microscopy. Nat. Nanotechnol., 2009, **4**, 186–192.

[2] Liess, C., Lüsse, S., Karger, N., Heller, M., Glüer, C.G., 2002. Detection of changes in cartilage water content using MRI T2-mapping in vivo. Osteoarthr. Cartil., 2002, **10**, 907–913.

[3] Kokkonen, H.T., Jurvelin, J.S., Tiitu, V., Töyräs, J., 2011. Detection of mechanical injury of articular cartilage using contrast enhanced computed tomography. Osteoarthr. Cartil., 2011, **19**, 295–301.

[4] Castro-Perez, J.M., Kamphorst, J., Degroot, J., Lafeber, F., et al., 2010. Comprehensive LC-MSE lipidomic analysis using a shotgun approach and its application to biomarker detection and identification in osteoarthritis patients. J. Proteome Res., 2010, **9**, 2377–2389.

[5] Park, Y.M., Han, Y.D., Kim, K.R., Zhang, C., Yoon, H.C., 2015. An immunoblot-based optical biosensor for screening of osteoarthritis using a smartphone-embedded illuminometer. Anal. Methods, 2015, **7**, 6437–6442.

[6] Park, Y.M., Kim, S.J., Lee, K.J., Yang, S.S., et al., 2015. Detection of CTX-II in serum and urine to diagnose osteoarthritis by using a fluoro-microbeads guiding chip. Biosens. Bioelectron., 2015, **15**, 192–199.

[7] Reijman, M., Hazes, J.M.W., Bierma-Zeinstra, S.M.A., Koes, B.W., et al., 2004. A new marker for osteoarthritis: Cross-sectional and longitudinal approach. Arthritis Rheum., 2004, **50**, 2471–2478.

[8] Garnero, P., Conrozier, T., Christgau, S., Mathieu, P., et al., 2003. Urinary type II collagen C-telopeptide levels are increased in patients with rapidly destructive hip osteoarthritis. Ann. Rheum. Dis., 2003, **62**, 939–943.

[9] Nomura, K., Gopinath, S.C.B., Lakshmipriya, T., Fukuda, N., et al., 2013. An angular fluidic channel for prism-free surface-plasmon-assisted fluorescence capturing. Nat. Commun., 2013, **4**, 2855.

[10] Gopinath, S.C.B., Tang, T.H., Chen, Y., Citartan, M., Lakshmipriya, T., 2014. Current aspects in immunosensors. Biosens. Bioelectron., 2014, **57**, 292–302.

[11] Lakshmipriya, T., Fujimaki, M., Gopinath, S.C.B., Awazu, K., 2013. Generation of anti-influenza aptamers using the systematic evolution of ligands by exponential enrichment for sensing applications. Langmuir, 2013, **29**, 15107–15115.

[12] Liu, F., Zhang, J., Chen, R., Chen, L., Deng, L., 2011. Highly effective colorimetric and visual detection of ATP by a DNAzyme-aptamer sensor. Chem. Biodivers., 2011, **8**, 311–316.

[13] Jin, N.Z., Gopinath, S.C.B., 2016. Potential blood clotting factors and anticoagulants. Biomed. Pharmacother., 2016, **84**, 356–365.

[14] Wang, H., Lakshmipriya, T., Chen, Y., Gopinath, S.C.B., 2019. Squamous Cell Carcinoma Biomarker Sensing on a Strontium Oxide-Modified Interdigitated Electrode Surface for the Diagnosis of Cervical Cancer. Biomed Res. Int., 2019, **2019**, 1–7.

[15] Guo, S., Lakshmipriya, T., Gopinath, S.C.B., Anbu, P., Feng, Y., 2019. Complementation of ELISA and an Interdigitated Electrode Surface in Gold Nanoparticle Functionalization for Effective Detection of Human Blood Clotting

Defects 2019, **14**, 222.

[16] Bourjilat, A., Sarry, F., Kourtiche, D., Nadi, M., 2018. Modelization of interdigitated electrode sensor for impedance spectroscopy measurement. Proc. Int. Conf. Sens. Technol. ICST, 2018, **2017**-**Decem**, 1–5.

[17] Sathya, S., Muruganand, S., Manikandan, N., Karuppasamy, K., 2019. Design of capacitance based on interdigitated electrode for BioMEMS sensor application. Mater. Sci. Semicond. Process., 2019, **101**, 206–213.

[18] Dziąbowska, K., Czaczyk, E., Nidzworski, D. Detection Methods of Human and Animal Influenza Virus—Current Trends**.** Biosensors (Basel). 2018 **8**, 94.

[19] Letchumanan, I., Md Arshad, M.K., Balakrishnan, S.R., Gopinath, S.C.B., 2019. Gold-nanorod enhances dielectric voltammetry detection of c-reactive protein: A predictive strategy for cardiac failure. Biosens. Bioelectron., 2019, **130**, 40–47.

[20] Bao, X., Huo, G., Li, L., Cao, X., et al., 2019. Coordinated Dispersion and Aggregation of Gold Nanorod in Aptamer-Mediated Gestational Hypertension Analysis. J. Anal. Methods Chem., 2019, **2019**, 5676159.

[21] Letchumanan, I., Gopinath, S.C.B., Md Arshad, M.K., Anbu, P., Lakshmipriya, T., 2019. Gold nano-urchin integrated label-free amperometric aptasensing human blood clotting factor IX: A prognosticative approach for “Royal disease.” Biosens. Bioelectron., 2019, **131**, 128–135.

[22] Parmin, N.A., Hashim, U., Gopinath, S.C.B., Rejali, Z., Afzan, A., 2019. A Sensitive DNA Biosensor using Screen Printed Gold Electrode Interdigitated Electrode (IDE) Pattern based for Identification of Human Papillomavirus Type 18 Variants 2019, **1**, 1–8.

[23] Zeng, S., Yong, K.T., Roy, I., Dinh, X.Q., et al., 2011. A Review on Functionalized Gold Nanoparticles for Biosensing Applications. Plasmonics, 2011, **6**, 491–506.

[24] Li, Y., Schluesener, H.J., Xu, S., 2010. Gold nanoparticle-based biosensors. Gold Bull., 2010, **10**, 18–33.

[25] Ramanathan, S., Gopinath, S.C.B., Md Arshad, M.K., Poopalan, P., et al., 2019. Assorted micro-scale interdigitated aluminium electrode fabrication for insensitive electrolyte evaluation: zeolite nanoparticle-mediated micro- to nano-scaled electrodes. Appl. Phys. A, 2019, **125**, 548.

[26] Kyaw, H.H., Al-Harthi, S.H., Sellai, A., Dutta, J., 2015. Self-organization of gold nanoparticles on silanated surfaces. Beilstein J. Nanotechnol., 2015, **6**, 2345–2353.

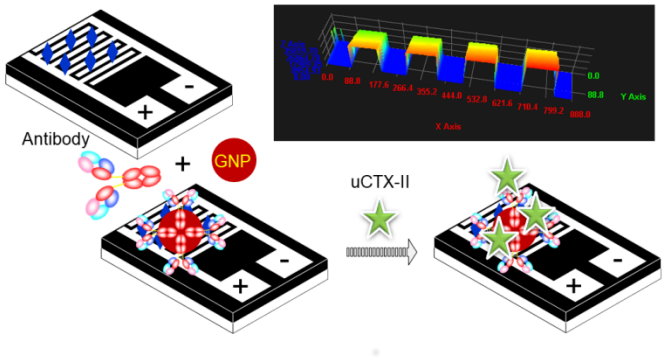

FIG. 1 Schematic illustration of detection of uCTX on IDE sensing surface. Antibody-conjugated GNP was immobilized on IDE surface though APTES as amine linker and determined the uCTX level. 3D nanoprofiling image is shown as inset.

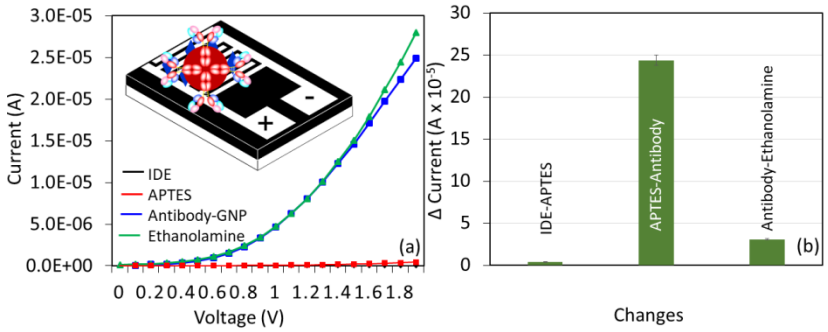

FIG. 2 (a) Immobilization process of antibody-GNP on IDE surface. GNP-conjugated antibody was immobilized on KOH-modified IDE surface through amine with APTES linker. Figure inset display the diagrammatic representation. (b) Current changes with antibody-GNP immobilization. Big difference of current changes was noted after immobilizing the antibody. Averaged the values by triplicates (n=3).

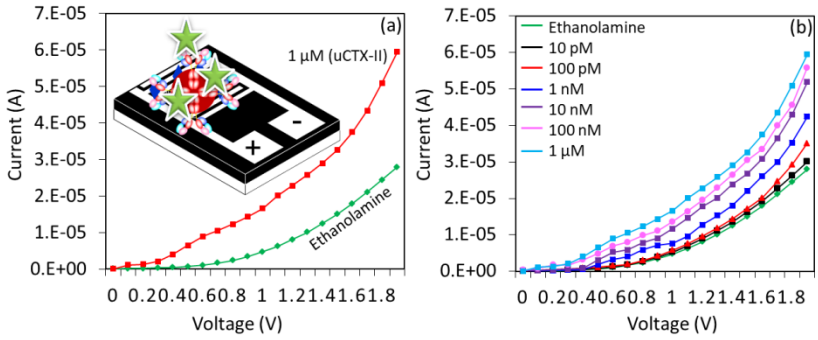

FIG. 3 Detection of uCTX on GNP-antibody modified surface. 1 µM of uCTX shows the clear difference in current increment indicating the interaction of uCTX with its antibody. Figure inset display the diagrammatic representation. (b) Detection limit of uCTX. uCTX concentrations from 10 pM to 100 nM were interacted independently on antibody-GNP modified surface. Clear current changes were noticed.

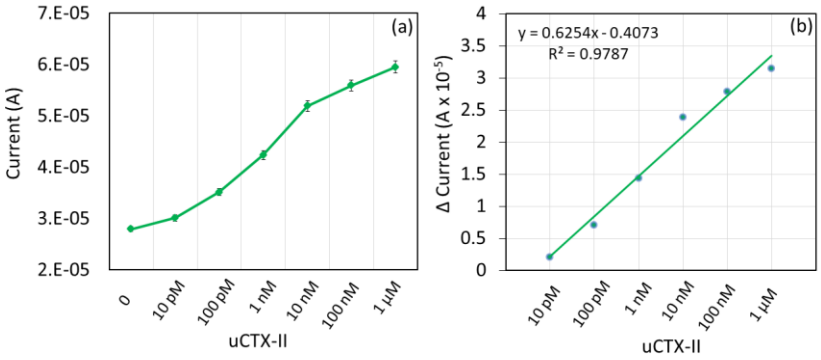

FIG. 4 (a) Current levels with different concentrations of uCTX with its antibody. With increasing the concentrations of uCTX, the current levels also were gradually increased. (b) Linear regression analysis with uCTX interaction with antibody. From the regression curve, the limit of detection was calculated in between the range of 10 and 100 pM.

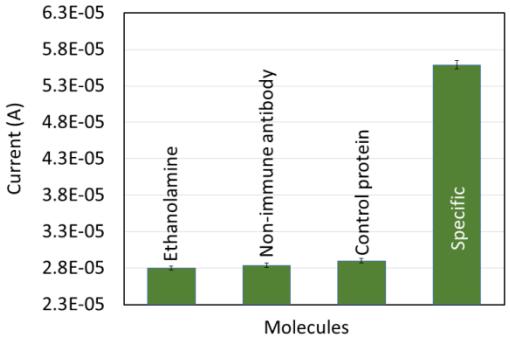

FIG. 5 Control experiments for specific detection of uCTX. Control experiment was performed with nonimmune antibody and albumin. Both experiments did not show any specific responses of current changes, indicating the specific detection of uCTX. Averaged the values by triplicates (n=3).